Appl. Sci. Converg. Technol. 25(5): 98-102 (2016)
http://dx.doi.org/10.5757/ASCT.2016.25.5.98

Research Paper

Full 3D Level Set Simulation of Nanodot Fabrication using FIBs

Heung-Bae Kim*
Department of Mechanical Engineering, Myongji College, Seoul 03656, Korea

Received August 5, 2016; accepted August 30, 2016

Abstract The level set method has recently become popular in the simulation of semiconductor processes such as etching, deposition and photolithography, as it is a highly robust and accurate computational technique for tracking moving interfaces. In this research, full three-dimensional level set simulation has been developed for the investigation of focused ion beam processing. Especially, focused ion beam induced nanodot formation was investigated with the consideration of three-dimensional distribution of redeposition particles which were obtained by Monte-Carlo simulation. Experimental validations were carried out with the nanodots that were fabricated using focused Ga^+ beams on Silicon substrate. Detailed description of level set simulation and characteristics of nanodot formation will be discussed in detail as well as surface propagation under focused ion beam bombardment.

Keywords: Focused ion beam, Microfabrication, Nanofabrication, Level set

I. Introduction

Sputtering is the fabrication of solid surface by bombardment with energetic ions. The amount of sputtered particles can be meaningful as sputtering yield, Y(θ), which is defined as the number of ejected atoms in solid by primary energetic incoming particle. Generally, the sputtering yield is a function of incident angle of incoming ion.

The sputtering has received remarkable attention due to its understanding is important in several disciplines such as the formation of thin films, surface technologies, cleaning of solid target in surface physics, etc [1-3]. Generally, when energetic ions bombard the solid surface, variety of ion-solid interactions, including sputtering, redeposition, swelling, implantation, backscattering, can occur. Simulation of ion beam induced physical and chemical phenomena, including topography changes, is essential in fabricating micro/nano structures [4-12]. In addition, redeposition is one of serious problem in accurate fabrication of certain structures. Many efforts have been made to understand ion beams induced fabrication processes. Especially, modeling and simulation are well established by several researchers [13-16].

A two-dimensional simple approximation of redeposition Zflux was reported by Orloff et. al. [17] as $\cos(\alpha)\cos(\beta)/d$. Here α and β are the emission and the incident angles of sputtered particles. Distance between source and destiny surface is represented by d.

A more accurate modeling and simulation related work was reported by Kim et al [13]. In the work, two-dimensional simulation with mathematical model of focused ion beam processing was established and verified by experimental. The three-dimensional Cosine distribution of redeposition flux was used. In the distribution of $f_{3D}=\cos^n(\alpha)$, preferential direction of sputtered atoms is controlled. If $n<1$ corresponds to side direction, whereas $n>1$ describes normal directions. For the purpose of two-dimensional simulation, three dimensional cosine distributions was normalized and projected onto two dimensional simulation domains. Otherwise simulation does not consider redeposition fluxes that are from all the other surface of ion irradiation. Constructed and un-constructed grid based full three dimensional simulations were performed with three-dimensional distribution of redeposition flux by Kim et al [14]. In addition, Kim et al. [15] reported two-dimensional level set simulation and demonstrated surface contact in focused ion beam TEM sample preparation. However sputtered atoms cosine index n was assumed to 1 in above mentioned simulation works. However some of angular distributions are well approximated by the rule. Exceptional examples are specular reflection and heart-shaped distributions. So accurate measurement or simulation is absolutely necessary as well as sputtering yield variations.

In this paper, full three-dimensional simulation method is presented. The simulation has been developed with level set mathematical scheme with the consideration of redeposition flux. Accurately predicted sputtering yields and sputtered atoms distributions that were obtained from famous Monte Carlo simulation software SRIM [18] are presented as well as its usage. Basic description and simulation results of level set method is discussed with

*Corresponding author
E-mail: heungbaekim@gmail.com

experimental validations.

II. Full Three Dimensional Level set Simulation

The level set method is one computational technique for tracking a propagating interface over time, which in many problems has proven more accurate in handling topological complexities as entropy conditions and weak solutions. The basic idea behind the level set method is to represent the surface at a certain time t as the zero level set of the so-called level set function Φ(t, x) as show in Figure. 1. The evolution of the level set function is determined by the velocities $v_{\perp}(x, t)$ of the surface point perpendicular to the surface. In the case of focused ion beam processing, the flux F of surface reaching particles (e.g., number of particles per time and surface area) causes surface movemont. Surface movement velocity is describes as $v_{\perp}$= F/N, where N is the atomic density of the target. The velocities of surface movement have to be calculated in the whole simulation surface as is discussed below.

In the level set method, time-dependent Hamilton-Jacobi and related equations is used to determine the surface at a certain time t by solving on fixed structured grids. One of the partial differential equation form is:

$$D_t\phi(x,t) = H(x,t,\phi,\nabla\phi,D_x^2\phi) = 0 \qquad x \in R^n, t \geq 0 \tag{1}$$

$D_t\Phi$ is the partial derivative of Φ with respect to the time variable t, $\nabla\Phi=D_x\Phi$ is the gradient of Φ, and $D^2_x\Phi$ is the Hessian matrix of the second partial derivatives with respect to the space variable. In focused ion beam simulation the speed of the surface Γ is calculated from external physics such as $v_{\perp}(x, t)$ as described previously. In general the speed function $v_{\perp}(x, t)$ of Γ represents the surface evolving speed of along its normal direction. The level set equation is described as:

$$D_t\phi(x,t) + v_{\perp}(x,t)|\phi(x,t)| = 0 \tag{2}$$

The initial condition Φ(x,t=0) is given by the signed distance function, i.e. the distance of the point x from the surface Γ, with a positive (negative) sign if the point is outside (inside) the surface. In addition, a necessary condition for the stability of this scheme is the Courant-Friedrichs-Levy (CFL) condition [19] which requires that

$$\Delta t \cdot v_{\perp} \leq min\Delta(\Delta x, \Delta y, \Delta z) \tag{3}$$

Where Δx, Δy, Δz, and Δt present the discretized steps in space and time, respectively.

To check the visibility between two points efficiently, the implicit representation of the interface of the level set function can be simply used. It is only needed to check whether Φ(x)>0 or not for all points on the line which connects source and target points.

During the every simulation step, these checks are performed at evenly spaced points on the connecting line between source and target. The values Φ can be obtained by interpolation at given point. The space between two points have to be carefully chosen smaller than the given grid spacing.

Generally the speed function is not defined on the whole simulation domain, because it has no clear physical meaning at certain points which are not on the feature surface. Therefore the speed function has to be extended from the known values on the surface to the whole simulation domain. Mathematically the general requirement for $v_{\wedge,ext}$ extension velocities is that

$$\lim_{x \to a} v_{\perp,ext}(x) = v_{\perp}(a) \tag{4}$$

Where a represents a point on the zero level set. In other words, the extension velocities must agree with the actual velocities as the surface is approached. The choice of extension velocities can directly influence the overall simulation efficiency of a surface evolution. When surface velocities are determined by complex techniques such as

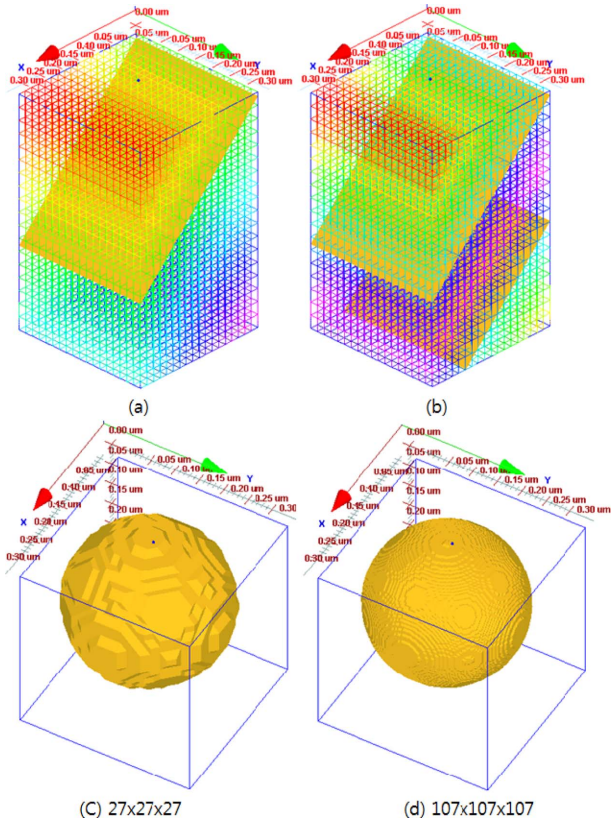

Figure 1. Level surfaces and corresponding level data structures (grids); (a) single zero level plane for the simulation of thick solid and (b) two zero level planes for the simulation of thin film membrane. Color maps in (a) and (b) represent level values and each level grid points. Representation of Spheres with coarse and fine level surface in three-dimensional space; 27(c) and 107(d) grids in each were used for the representations.

fast marching the time required for level set calculations is reduced dramatically.

The first step of the level set calculation is to establish a grid points that construct the initial surface. Generally, the finer the grid spacing the more accurate the level-set results can be obtained. Level grids have to be coarse enough to represent initial level surface. As shown in Figure. 1(c) and (d) the more grids the coarser level surface will be. However, as mentioned before, computation time is increase as increase grids.

For the simulation of the ion beam induced surface evolution, accurate value of sputtering yield has to be obtained in an accurate manner. The yield is a function of given incident angles, ion species, incidence energy, and substrate. Usually, Monte Carlo simulation is used to calculate sputtering yields according to the incident angles. One of the Monte Carlo simulation software tool, SRIM [18], has been used for calculating the sputtering yield. Whereas, TRIDYN [20] is capable of calculating the changes of the target composition which is caused by implanted ions during sputter process.

In addition to sputtering yields, one of serious problem in using focused ion beam is redeposition which is generated spontaneously by ion bombardment of target solids. The redeposited atoms cause surface un-predictable so that

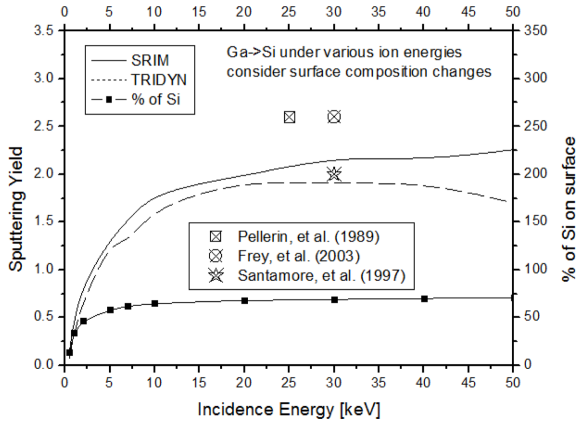

Figure 2. Sputtering yield of Si as a function of ion energies. Yields were obtained from SRIM and TRIDYN with Ga^+ [21-23].

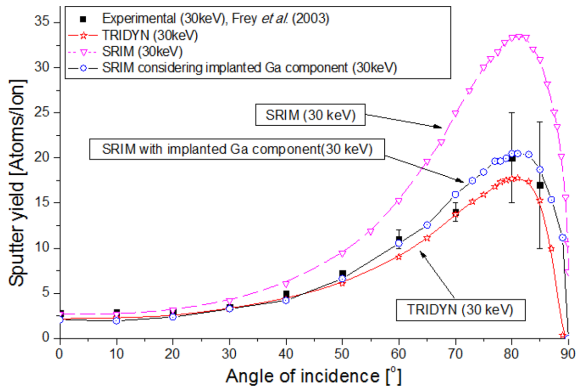

Figure 3. Comparison of sputtering yields with experimentally obtained yields. Experiments are from Ref. [22].

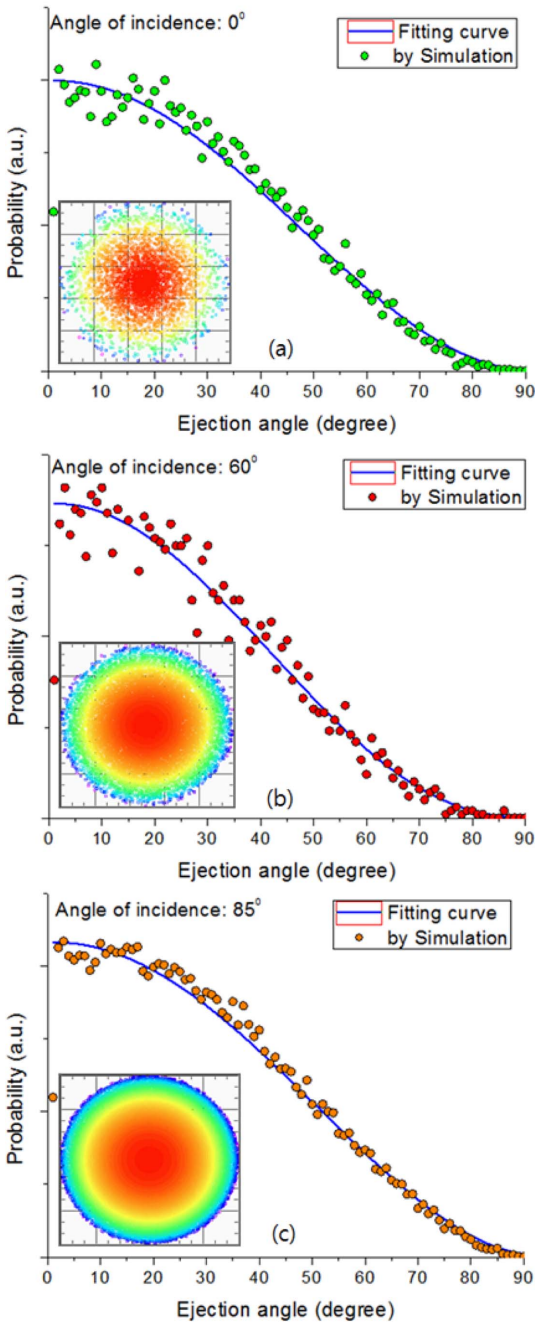

Figure 4. Simulated probability distribution of sputtered atoms at incident angles of (a) 0°, (b) 60 and (c) 85°. Probabilities are fitted with cosine function with power of n ((a) n=2.3, (b) n=2.1 and (c) n=1.7). The insets at each figure are top view of sputtered atoms distributions gathered at half-sphere. The color map represent emission angle of sputtered particles (Red (0^o) to Violet (90^o) measured from surface normal direction).

accurate fabrication is not attainable without knowledge about them. Several efforts have been made so far and recently redeposition is well modeled and simulated with good accuracy. The three-dimensional distribution of redeposition flux is usually described by cosine function. $f_{3D}=\cos^n(\alpha)$.

In the previous works, TRIDYN was mainly used to calculate the sputtering yields because it consider implanted

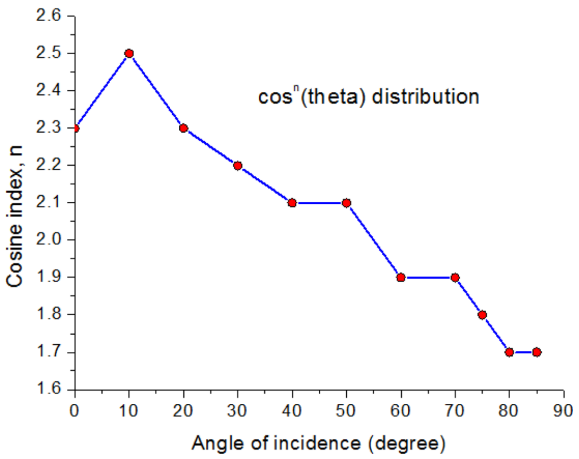

Figure 5. Simulated and fitted cosine indexes n as function of angle of incidence. Incident angle of 90 was not calculated due to the assumption of zero sputtering yields.

incident ion component (e.g. Ga component). The distribution of redeposition fluxes were modeled simply with cosine index n=1. However, TRIDYN code is not easily obtainable compare to SRIM which can be simply downloaded in the Web[18]. In this work, the sputtering yields and the distribution were calculated with SRIM with some modification of input value. Figure. 2 shows Ga components changes and sputtering yields as a function of incidence energies. It shows that 25% of Ga component were implanted in silicon substrate at energies over 10 keV. Therefore, accurate sputtering yield and sputtered atoms distribution can be obtained by inputting 25% and 75% of Ga and Si compositions using SRIM code. Heat of sublimation of 4.7 and 2.82 eV for Si and Ga components are additionally necessary as well as corrected density.

In the SRIM simulation, 1000 Ga ions were used for the simulation with silicon substrate. As results, the sputtering yields by SRIM are well suited to values obtained from experiments compared to TRINDYN as shown in Figure. 3. The distributions of sputtered atoms were fitted with $\cos^n(\alpha)$ for the calculation of index n as function of incidence angles as Figure. 4 and 5.

III. Experiment

For the comparison of simulated and experimentally obtained nanodot, previously reported experimental data were adapted as shown in Figure. 6. The dot was fabricated using a Micrion 2500 with a gallium ion source (LMIS). The system was operated at an acceleration voltage of 50 kV with a beam current of 45 pA. A silicon substrate used with the beam diameter of 68 nm in FWHM and the current density was 0.8 Acm^2 at the Gaussian beam center. The ion dose was 0.5 pC in exposure times of 0.011(s). Then the surface profiles of the fabricated structures were obtained with atomic force microscopy with a small tip radius about 10 nm.

IV. Results and Discussion

Overlapped between two experimental and simulated dot indicates that maximum depth of simulated dot is well predict experimental one (Figure. 6(a)) besides sidewall formation cannot be comparable due to shallow depth of dot. A simulation with more ion irradiation time is depicted in Figure. 6(c). However, additional experiments of more ion irradiation time are necessary for the purpose of redeposition flux contribution of side wall formation in nanodot formation.

Additional experiments were carried out using a FEI NOVA 200 Dualbeam system equipped with a Gallium ion source and field emission scanning electron microscope (FESEM). An acceleration voltage of 30 kV and a beam current of 48 pA were used.

After the fabrication, the focused ion beam cross-sectioned surface was investigated with a scanning electron microscope with 52° tilting angle to the cross section surface. The beam diameter in FWHM was 125 nm (e.g. blur was applied for the easy investigation with bigger dot diameter) and the current density at the center was 0.26 Acm^2. Overlapped results are in Figure. 7 with simulation results. Exposure times of 0.1 (Figure. 7(a)) and 0.12s (Figure. 7(c)) were applied for the formation of dots. The maximum depths of the dots were 64 nm and 88 nm, respectively.

The excellent agreements between simulations and experimental were observed. In addition, surface diffusion plays a minor role during the focused ion beam induced nanodot formation. However, reflection of ion at the higher incident angle is not considered in the model, some deviations are originally taken place in the simulations.

Simulation results those exposure times of 0.1s to 0.16s in step of 0.02s are shown in Figure. 8(a-e). An additional simulation result without considering redeposition flux is presented in Figure. 8(f). If the two-dimensional simple approximation of redeposition flux reported by Orloff et al [17] was used for the simulation, one may obtain the same

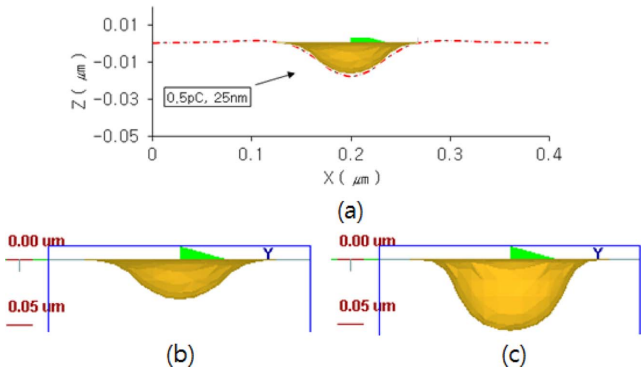

Figure 6. Overlap of experimentally obtained and simulated profiles (a) and simulated results of nano dot formation (b and c). The dot was milled with Ga+ and incidence energy of 30 keV[14] and the profiles was measured with AFM. The measured and simulated depths are 25 nm and 30 nm, respectively.

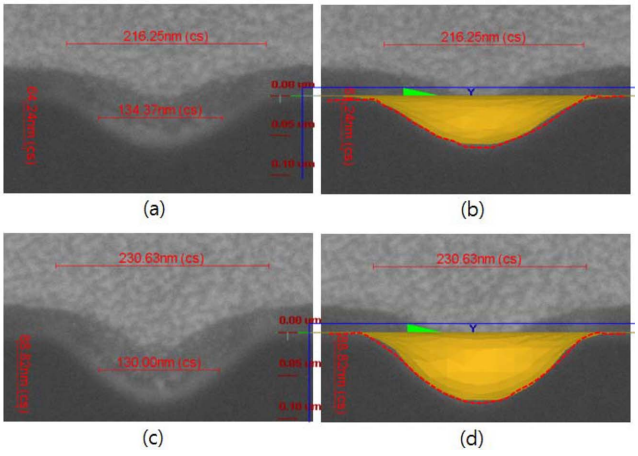

Figure 7. Experimentally obtained SEM images of cross-section of focused ion beam milled single pixel nanodot. Exposure times are 0.1(a) and 0.12s (c) with the maximum current density of 0.12 Acm^{-2} at the center of the beam. The images are tilted 52°. Simulation results are overlapped with the experimental with rescale by tilting angle. Red dotted curves in (b) and (d) correspond to experimentally obtained contours in (a) and (c), respectively.

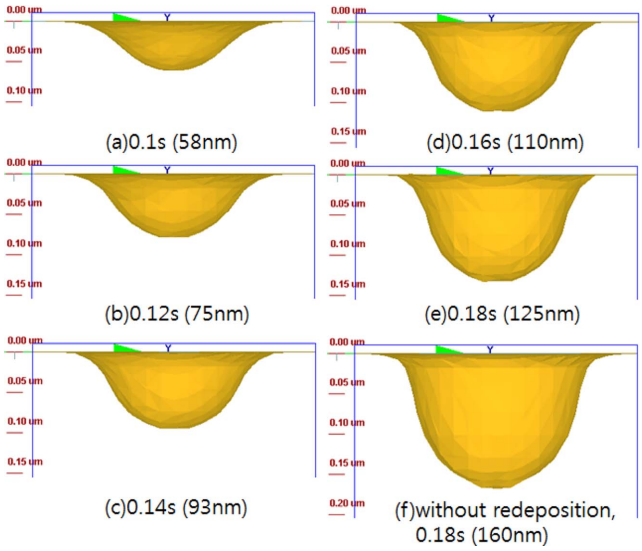

Figure 8. Simulation results of nanodot. From (a) to (c) are correspond to (a) to (c) in Figure. 7. Additional milling simulation with more exposure times are shown from (c) to (e). Simulation result without considering of redeposition fluxes is in (f). Exposure times and maximum depths are depicted in the below of individual result.

results in Figure. 8(f). However, fundamentally Orloff's approximation cannot be directly used to simulate rotationally symmetric three-dimensional shape such as single nanodot or pillar-like structures without normalization and consideration of all the surfaces ion irradiation (e.g. projection of redeposition fluxes onto two dimensional simulation space).

V. Conclusions

This paper presented full three-dimensional level set simulation results. The simulation were performed under sound mathematical scheme with level set method. To consider the redeposition flux, distributions of sputtered particle were calculated with Monte-Carlo simulation code SRIM. The Ga ion component which is implanted into the substrate was considered in the Monte-Carlo simulation. A series of experiments were performed to verify accuracy of the level-set simulation. Single pixel millings of nanodot were fabricated and compared with the simulation results. The simulation results well agreed with the experimental so that the simulation and the distribution of sputtered particles as well as sputtering yield were proved to be well estimated.

The level set simulation can be used to plan focused ion beam utilized microfabrication process especially for redeposition induced shape variations.

References

[1] A. A. Tseng, J. Micromech. Microeng. 14, R15 (2003).
[2] S. Reyntjens and R. Puers, J. Micromech. Microeng. 11, 287 (2001).
[3] R. Young, Vacuum 44, 353 (1993).
[4] M. J. Vasile, Z N Nassar, and S. Liu, J, Vac, Sci, Technol B 15, 2350 (1997).
[5] M. J. Vasile, J. Xie, and R. Nassar, J. Vac. Sci. Technol. B 17, 3085 (1999).
[6] D. P. Adams and M. J. Vasile, J. Vac. Sci. Technol. B 24, 836 (2006).
[7] D. P. Adams, M. J. Vasile, and T. M. Mayer, J. Vac. Sci Technol. B 24, 1766 (2006).
[8] Y. Fu and N. K. A. Bryan, J. Vac. Sci. Technol. B 22, 1672 (2004).
[9] H. B. Kim, G. Hobler, A. Steiger, A. Lugstein, E. Bertagnolli, E. Platzgummer, and H. Loeschner, Int. J. Precis. Eng. Manuf., 12, 893 (2011).
[10] H. B. Kim, Micromech. Microeng. 88, 3365 (2011).
[11] H. B. Kim, Micromech. Microeng. 91, 14 (2012).
[12] H. B. Kim, G. Hobler, A. Steiger, A. Lugstein, and E. Bertagonolli, Opt. Exp. 15, 9444 (2007).
[13] I. V. Katardjiev, J. Vac. Sci. Technol. A6, 2434 (1998).
[14] H. B. Kim, G. Hobler, A. Lugstein, and E. Bertagonolli, J. Micromech. Microeng. 17, 1178 (2007).
[15] H. B. Kim, G. Hobler, A. Steiger, A. Lugstein, and E. Bertagonolli, Nanotechnology 18, 245303 (2007).
[16] H. B. Kim, G. Hobler, A. Steiger, A. Lugstein, and E. Bertagonolli, Nanotechnology 18, 265307 (2007).
[17] J. Orloff, CRC Press, 549 (2009).
[18] F. Ziegler, http://www.srim.org , (2003)
[19] J. A. Sethian, Combridge University Press, (1999).
[20] W. Moeller and M Posselt, Dresden, Forschungszentrum Rossendorf , (2002).
[21] L. Frey, C. Lehrer, and H. Ryssel, Appl. Phys. A 76, 1017 (2003).
[22] J. Pellerin, D. Griffis, and P. Rusell, J. Vac. Sci. B 8, 1949 (1990).
[23] D. Santamore, K. Edinger, J. Orloff, and J. Melngailis, J. Vac. Sci. Technol. B 15, 2346 (1997).